



Published in final edited form as:

Oncogene. 2020 June ; 39(23): 4581–4591. doi:10.1038/s41388-020-1320-6.

The Crucial p53-Dependent Oncogenic Role of JAB1 in Osteosarcoma *in vivo*

William E. Samsa^{1,2}, Murali K. Mamidi^{1,2}, Lindsay A. Bashur¹, Robin Elliott³, Alexander Miron^{2,4}, Yuqing Chen⁵, Brendan Lee⁵, Edward M. Greenfield⁶, Ricky Chan⁷, David Danielpour^{2,8}, Guang Zhou^{1,2,4}

¹Case Western Reserve University, Department of Orthopaedics

²Case Western Reserve University, Case Comprehensive Cancer Center

³Case Western Reserve University, Department of Pathology

⁴Case Western Reserve University, Department of Genetics and Genome Sciences

⁵Case Western Reserve University, Department of Molecular and Human Genetics, Baylor College of Medicine

⁶Case Western Reserve University, Indiana University School of Medicine

⁷Case Western Reserve University, Case Comprehensive Cancer Center, Institute for Computational Biology

⁸Case Western Reserve University, Division of General Medical Sciences

Abstract

Osteosarcoma (OS) is the most common primary bone cancer and ranks amongst the leading causes of cancer mortality in young adults. Jun activation domain binding protein 1 (*JAB1*) is overexpressed in many cancers and has recently emerged as a novel target for cancer treatment. However, the role of *JAB1* in osteosarcoma was virtually unknown. In this study, we demonstrate that *JAB1*-knockdown in malignant osteosarcoma cell lines significantly reduced their oncogenic properties, including proliferation, colony formation, and motility. We also performed RNA-sequencing analysis in *JAB1*-knockdown OS cells and identified 4110 genes that are significantly differentially expressed. This demonstrated for the first time that *JAB1* regulates a large and specific transcriptome in cancer. We also found that *JAB1* is overexpressed in human OS and

Users may view, print, copy, and download text and data-mine the content in such documents, for the purposes of academic research, subject always to the full Conditions of use:http://www.nature.com/authors/editorial_policies/license.html#terms

Corresponding Author: Guang Zhou, Biomedical Research Building, #328, 2109 Adelbert Rd, Cleveland, OH, 44106, (216) 368-2260, gxz27@case.edu.

Authors' Contributions

Conception and design: W.E. Samsa, G. Zhou

Development of methodology: W.E. Samsa, M. K. Mamidi, L. A. Bashur, Y. Chen, B. Lee, E. Greenfield, D. Danielpour, G. Zhou

Acquisition of data: W. E. Samsa, M. K. Mamidi, L. A. Bashur, R. Elliott, A. Miron, E. Greenfield, G. Zhou

Analysis of data: W. E. Samsa, M. K. Mamidi, L. A. Bashur, R. Elliott, R. Chan, D. Danielpour, G. Zhou

Writing of the manuscript: W. E. Samsa, M. K. Mamidi, D. Danielpour, G. Zhou

Study supervision: W. E. Samsa, G. Zhou

Disclosure of Competing Financial Interests

The authors declare no competing financial interests.

Supplementary information is available at *Oncogene*'s website

correlates with a poor prognosis. Moreover, we generated a novel mouse model that overexpresses *Jab1* specifically in osteoblasts upon a *TP53* heterozygous sensitizing background. Interestingly, by 13 months of age, a significant proportion of these mice spontaneously developed conventional OS. Finally, we demonstrate that a novel, highly specific small molecule inhibitor of JAB1, CSN5i-3, reduces osteosarcoma cell viability and has specific effects on the ubiquitin-proteasome system in OS. Thus, we show for the first time that the overexpression of *JAB1 in vivo* can result in accelerated spontaneous tumor formation in a p53-dependent manner. In summary, JAB1 might be a unique target for the treatment of osteosarcoma and other cancers.

Keywords

JAB1/CSN5/COPS5; p53; Osteosarcoma; Osteoblast; Oncogenesis

Introduction

Osteosarcoma (OS) is the most common primary bone cancer that predominately affects adolescents and causes the third most cancer-related deaths in young adults (1). Human genetic studies identified various germline mutations associated with an increased incidence of osteosarcomas, such as Li-Fraumeni *TP53* mutations and Retinoblastoma *RB1* mutations (2). Current osteosarcoma treatment consists of chemotherapy and aggressive surgical resection; however, the 5-year survival rate remains at only 70%, which is further reduced to as low as 20% in patients with metastases (1, 2).

Osteosarcoma is characterized by a complex karyotype with high-level genomic instability (2). Furthermore, a lack of mouse models renders the study of OS initiation and pathogenesis challenging. However, based on human and mouse genetic studies, mutant *TP53* emerged as a major driver of OS formation (3, 4). Mice with a heterozygous deletion of *Tp53* develop osteosarcoma with ~25% incidence rate by 18 months of age, and mouse models with the mesenchymal cell lineage-specific disruption of *Tp53* and *Rb* results in osteosarcoma formation with a higher penetrance and a shorter latency (3–7). Thus, TP53 is the main driver of OS development.

Jun activation domain-binding protein 1 (JAB1), also known as COP9 signalosome subunit 5 (CSN5/COPS5), is the fifth and enzymatic subunit of the highly conserved macromolecular complex, the COP9 Signalosome (CSN) (8). The importance of the CSN is underscored by the fact that the deletion of any individual subunits, CSN1-8, in mice, results in early embryonic lethality (8, 9). The CSN plays an important role in the regulation of protein turnover through its ability to cleave NEDD8, a small ubiquitin-like protein, from the active form of the largest family of E3 ubiquitin ligases, the Cullin-RING ligases (CRLs), thus inactivating them (8, 10). Intriguingly, *Jab1* has been shown to play an essential role in cellular differentiation, cell cycle regulation, apoptosis, and DNA damage repair (9, 11–15). Indeed, our previous studies have demonstrated that *Jab1* is required for the successive stages of skeletogenesis (12, 13). Interestingly, JAB1 is also overexpressed in many human cancers, including breast and prostate cancer (9). Mechanistically, JAB1 is capable of inactivating several tumor suppressors, including p53 (16). However, the role of *Jab1* in

osteosarcoma pathogenesis *in vivo* was unknown until this study. Here, we report that *JAB1* is overexpressed in human osteosarcoma patient biopsy samples, and that the knockdown of *JAB1* in highly malignant human OS cancer cell lines reduces their oncogenic properties. We identified a large and specific *JAB1*-regulated transcriptome in OS. We also report for the first time that the *in vivo* overexpression of *Jab1* in mice specifically in osteoblasts results in accelerated spontaneous osteosarcoma formation in a p53-dependent manner.

Results

The knockdown of *JAB1* reduces osteosarcoma oncogenic properties.

To investigate the effect of the loss of *JAB1* on tumorigenesis, we performed lentiviral shRNA knockdowns in 143B and U2OS cells, two highly malignant human osteosarcoma cell lines (17, 18). As for *TP53* status, 143B harbors a R156P mutation and U2OS cells has wild-type *TP53* (19). We performed experiments using a scrambled control shRNA and at least 2 shRNAs specifically targeting *JAB1/COPS5* (Figure 1A and B). Similarly to what was reported in hepatocellular carcinoma, the loss of *JAB1* in 143B cells had relatively little effect on the protein abundance of COPS3, a potential driver gene in OS (20–22), and COPS8, a subunit linked to gastric cancer (23, 24) (Figure S1). To further determine the effect of *JAB1* loss on OS oncogenic properties, we performed standard functional assays in 143B and U2OS cells. Our colony formation results indicate that *JAB1*-knockdown cells had a significantly reduced number of crystal violet stained colonies in 143B (64.6 vs. 6.4) and in U2OS: (90.3 vs. 31.7) (Figure 1C), (Figure S2). The MTT assay demonstrated significantly reduced cell viability after 48 hours in 143B and U2OS cells (Figure 1D). Finally, the *in vitro* wound assay demonstrated that *JAB1* loss inhibits cell migration (Figures 1E and S3). *JAB1* silencing in LM7 cells, another highly metastatic OS cell line in which *TP53* is deleted, resulted in a similar functional defect (Figure S3) (19).

RNA-sequencing reveals that *JAB1* regulates a unique oncogenic transcriptome in OS.

Next, we sought to obtain an unbiased *JAB1*-mediated transcriptome in OS to gain insights into the underlying mechanism of *JAB1*-mediated OS pathogenesis using RNA-sequencing in 143B *JAB1*-knockdown cells. Upon *JAB1* depletion, there were a total of 4110 genes significantly differentially expressed, with 37.4% of those genes downregulated, and 62.6% upregulated (Figure 2A). Principal Component Analysis revealed that there is a very distinct set of genes that are dysregulated upon *JAB1* silencing (Figure 2B).

Next, we submitted the lists of both significantly upregulated and downregulated genes to the Database for Annotation, Visualization, and Integrated Discovery (DAVID) (25, 26). Figures 2C and 2D list the top 5 most significantly altered Gene Ontology (GO) terms regarding molecular functions, cellular components, and biological processes. Among the downregulated genes, a large number are involved in protein binding for molecular function, and their cellular components are mainly in the cytoplasm and cytosol (Figure 2C). The most significantly downregulated biological processes are involved in mitosis, cell cycle progression, and cell-cell adhesion (Figure 2C). In contrast, the cellular component of the upregulated genes is mainly localized in the nucleus, and interestingly, the molecular function of the upregulated genes is also mainly involved in protein binding (Figure 2D).

This overall finding is consistent with the well-established role of JAB1 in binding to a diverse set of proteins (9, 10). Next, we performed standard Gene Set Enrichment Analysis (GSEA) to identify the key biological pathways that are regulated by *JAB1* in OS (Figures 3A and 3B). GSEA using the HALLMARK gene sets of the Molecular Signature Database demonstrated that the cell cycle regulation was among the most downregulated pathways upon *JAB1*-knockdown (Figure 3A and Table S1). Moreover, the G2/M Checkpoint and E2F Targets pathways, which are part of the Rb/E2F network involved in controlling cell cycle progression and OS pathogenesis (27), is significantly altered. Furthermore, the DNA Repair and p53 pathways were also changed upon *JAB1*-knockdown (Figure 3B). Therefore, GSEA identified very similar pathways as DAVID analysis in *JAB1*-knockdown cells, particularly the cell cycle regulation among the downregulated genes, suggesting this is among the key JAB1 downstream pathways in OS (Tables S1 and S2).

The knockdown of *JAB1* impairs cell cycle progression, increases apoptosis, and its overexpression in human osteosarcoma is correlated with poor prognosis.

To determine the effect of the *JAB1* loss on cell cycle progression, we conducted flow cytometry analysis in *JAB1*-knockdown 143B cells. There were significant changes in the percentage of cells at each phase of the cell cycle (Figure 4C). Cyclin A2 plays an important role in the G2/M phase transition, and is a common marker of cell proliferation (28). Cyclin B1 is important for entry into mitosis (29). The levels of these two cyclins were downregulated, indicating impaired cell cycle progression upon *JAB1*-knockdown (Figure 4C). The most striking change in our flow cytometry analysis was the large increase in the percentage of cells in the sub G0 phase, suggesting an increased number of apoptotic cells (Figure 4C). Indeed, our GSEA analysis also identified an increase in the apoptosis pathway (Figure 4D). Notably, the levels of BAX, a key pro-apoptotic Bcl-2 family member, was increased upon *JAB1*-knockdown in 143B cells (Figure 4E). Furthermore, there was no change in the expression of BAK, another key pro-apoptotic Bcl-2 family member, and an increase in anti-apoptotic BCL-2 upon *JAB1*-knockdown (Figure 4D). Densitometry analysis revealed that there was an increased ratio of BAX:BCL-2, a key metric of apoptotic activity, in *JAB1*-knockdown 143B cells, indicating increased apoptosis and that BAX might be the major effector. Next, an unbiased screening identified 28 out of 45 of the most common signaling reporters being clearly altered (Figure 4F and Supplementary Table S3). These results indicate that *JAB1*-knockdown likely increases apoptosis and alters multiple major signal transduction pathways in OS cells.

JAB1 was previously reported to be overexpressed in many cancer cell types (9). Thus, we conducted JAB1 immunostaining using a tissue microarray containing human OS biopsy sections from 51 different osteosarcoma patients (Figure 4A). Interestingly, the quantification of the staining revealed that greater than 75% of the OS samples had high intensity staining (a score of 2 or 3) (Figure 4B). Of the 19 OS samples that received a staining score of 3, only 5 of them survived (Figure 4B). In contrast, JAB1 expression in normal bone was much weaker (Figure 4A). Thus, JAB1 is likely overexpressed in human osteosarcoma and might be correlated with poor survival outcomes.

The overexpression of *JAB1* in mice results in accelerated spontaneous bone tumor formation in a *p53*-dependent manner.

To date, *JAB1*-mediated animal tumor models are still very much lacking. To understand the role of *JAB1* in oncogenesis *in vivo*, we generated a novel mouse model that overexpresses *Jab1* specifically in osteoblasts (Figure 5A–B) (30). The *Coll1a1-Jab1* transgenic mice exhibited no obvious growth abnormalities and no tumor formation (Figure 5D). Both human and mouse genetic studies have identified mutant *Tp53* as the most prominent driver of OS development (2). Thus, we crossed our two *Coll1a1-Jab1* transgenic mouse lines (Tg#1 and Tg#2) with *Tp53* heterozygous mice. The *Coll1a1-Jab1; p53^{+/-}* mice were viable and indistinguishable from littermates prior to weaning age. However, by 13 months of age, these mice developed spontaneous bone tumors with a 30.4% penetrance (Figures 5C and 5D). The average age of tumor onset for *Tg#1; p53^{+/-}* and *Tg#2; p53^{+/-}* was 408 days and 392 days, respectively, with a range of 293–449 days. In contrast, only two *p53^{+/-}* mice developed osteosarcomas by 331 days and 541 days of age respectively. In both *Coll1a1-Jab1; p53^{+/-}* transgenic lines, the osteosarcomas were nearly evenly distributed between the hindlimb and forelimb (Figures 5D and 6A–D). Moreover, X-Ray analysis revealed mineral deposition in the tumors dissected from these limbs (Figure 6E–I). Overall, the tumors were conventional OS with hypercellularity. They can be categorized into osteoblastic and fibroblastic, but not chondroblastic, osteosarcomas (Figure 6J–N). Interestingly, in *JAB1*-knockdown 143B cells, the HALLMARK Epithelial Mesenchymal Transition pathway was significantly downregulated, suggesting that *JAB1* might be involved in EMT-mediated metastasis (Figure 6R). In support of this, some spontaneous osteosarcomas in *Coll1a1-Jab1; p53^{+/-}* mice displayed local invasion into the surrounding tissue, including the muscle and fat, but not into the nerves (Figures 6O–6Q). This is very similar to a mouse model of NOTCH-mediated OS (31). Additionally, *SNAI1*, a transcription factor that induces EMT, is decreased upon *JAB1*-knockdown in 143B cells (Figure 6R). Thus, the osteoblast-specific overexpression of *JAB1* accelerates spontaneous OS formation in mice in a *p53*-dependent manner, and may promote EMT.

JAB1 is a potential therapeutic target for OS treatment.

The NEDDylation pathway is known to trigger the activation of the largest family of E3 ubiquitin ligases, the Cullin-RING ligases (CRLs) (32). As illustrated in Figure 7A, the NAE1 (NEDD8-Activating Enzyme E1 Regulator Subunit) initiates the NEDDylation and activation of CRLs through the addition of an ubiquitin-like protein NEDD8, in a cascade analogous to ubiquitin transfer. On the other hand, *JAB1* is solely responsible for catalyzing the removal of NEDD8 from CRLs, thus deactivating CRLs and maintaining their cellular homeostasis (Figure 7A) (32). In recent years, the NEDDylation pathway has emerged as an attractive therapeutic target for cancer treatment (Figure 7A) (33–35). Indeed, MLN4924, a specific inhibitor of NAE1, is currently in clinical trials for the treatment of various cancers (35). Moreover, recently a highly specific small molecule inhibitor of *JAB1*, CSN5i-3, has been developed (36). CSN5i-3-mediated *JAB1* inhibition reduced cell viability in a large panel of cell lines, as well as repressed the growth of lymphoma xenografts in mice (36), but CSN5i-3's effects in OS have not been studied. Thus, we treated 143B OS cells and, as a control, human fetal osteoblasts (hFOBs) with CSN5i-3 and MLN4924 to determine if disrupting the NEDDylation pathway can prevent OS cell growth. Indeed, both drugs

inhibited OS cell growth in a dose-dependent manner, and 143B OS cells were more sensitive than hFOB3 to both CSN5i-3 (3.5 μ M vs 6.6 μ M) and MLN4924 (0.46 μ M vs. 14 μ M) (Figures 7C and 7E). Additionally, we generated three-dimensional multicellular tumor spheroids (sarcospheres) and determined their IC50 after 48 hours of treatment with CSN5i-3 (Figure 7D). This clonal, non-adherent, self-renewing, cancer stem cell like-model more closely represent the *in vivo* microenvironment, and better correlates with the *in vivo* response to chemotherapy when compared with monolayer cultures (18). Interestingly, our results demonstrate that 143B sarcospheres are more sensitive to treatment with CSN5i-3, with an IC50 of 2.9 μ M (Figures 7D and 7E). In CSN5i-3 treated cells, as expected (32, 36), the amount of the NEDDylated forms of CUL1 and CUL4A/B had increased, whereas in contrast, the expression of CUL1 and CUL4A/B in MLN4924-treated cells were completely abolished (Figure 7B). We also examined the expression of FBXO22, a poorly characterized F-box protein that plays a role in substrate specificity of CRL complexes (37). Similar to a previous report in a colon cancer cell line (36), FBXO22 levels were also completely abolished in CSN5i-3-treated OS cells, but unchanged in MLN4924-treated OS cells (Figure 7B). The expression of SKP2, another F-box protein that plays an important role in cell cycle progression (37), decreased in CSN5i-3-treated OS cells but increased in MLN4924-treated OS cells (Figure 7E). These data suggest that JAB1 might be a potential therapeutic target for OS, and FBXO22 might be a unique CSN5i-3 downstream target in diverse cancer cell types.

Discussion

In this study, for the first time, we demonstrate that *JAB1*-knockdown in metastatic osteosarcoma cell lines led to reduced oncogenic properties, with significantly reduced proliferation, colony formation, and motility. We also showed for the first time by RNA-sequencing that there exists a large *JAB1*-mediated oncogenic transcriptome in OS cells. Additionally, we show for the first time that in human OS patient biopsy samples, JAB1 is overexpressed in more than 75% of patients, and that there is likely a positive correlation between *JAB1* expression levels and OS mortality (Figure 4B). Most importantly, we also show for the first time that *JAB1* overexpression specifically in osteoblasts in mice on a *p53*^{+/-} sensitizing background results in an accelerated spontaneous bone tumor formation. Finally, for the first time, we demonstrate that *JAB1* might be a target for OS treatment using CSN5i-3, a novel, specific, and potent small molecule inhibitor of JAB1. Thus, our results strongly suggest that *JAB1* might be a diagnostic and prognostic biomarker for osteosarcoma, and that *JAB1* is a promising therapeutic target for treating osteosarcomas.

Gene ontology analysis of our RNA-seq dataset demonstrates that the molecular function of a significant number of the differentially expressed genes in *JAB1*-knockdown cells are involved in protein binding (Figures 2C and 2D), which is consistent with the well-established function of JAB1 in interacting with many other proteins (9). Moreover, GSEA analysis confirmed that *JAB1* regulates important oncogenic pathways, including the p53 pathway, Rb pathway, cell cycle arrest, DNA repair, and cell-cell adhesion (Figure 3). Interestingly, JAB1 expression has previously been linked to radiation sensitivity and DNA damage repair in OS *in vitro* (38). However, the underlying mechanism of *JAB1*'s role in these processes remains to be determined.

Our results demonstrate for the first time that *Jab1* overexpression results in spontaneous OS formation in a p53-dependent manner in mice. The low penetrance of tumor formation in this model is likely due to the low-level *Jab1* transgene expression achieved in osteoblasts. Interestingly, a previous study also reported that it was very challenging to achieve high-level *Jab1* expression *in vivo* (39). Therefore, generating a mouse model with high-level *Jab1* expression will be essential to further address the role of *Jab1* in tumorigenesis in whole animals.

In this study, we also provide evidence that JAB1 may be a suitable therapeutic target for clinical intervention in OS. The JAB1-containing COP9 Signalosome is an essential regulator of Cullin-RING Ligases (CRLs), which are central mediators of oncogenesis (8). CRL homeostasis is tightly regulated by NEDDylation (Figure 7A). A small molecule inhibitor of NAE1, MLN4924 (Figure 7A), inhibited tumor xenografts in mice, and is currently in many Phase I and II clinical trials for the treatment of hematologic and other cancers, as well as a phase III clinical trial in combination with azacitidine for the treatment of acute myeloid leukemia, but is associated with severe side effects, serious adverse events, and drug resistance (33–36, 40). CSN5i-3 is a recently developed and highly specific small molecule inhibitor of JAB1 (36). In contrast to the global inhibition of protein degradation by pan proteasome inhibitors, or the broad effect of inactivating all CRLs using MLN4924, CSN5i-3 might offer greater specificity, and therefore likely reduced side effects, due to its inactivation of only a subset of CRLs (36, 41). In this study, for the first time, we investigated the effect of both MLN4924 and CSN5i-3 on OS cells (Figure 7). We demonstrate that CSN5i-3 reduces OS cell viability, and that OS cells are more sensitive to treatment with both CSN5i-3 and MLN4924 compared with a human fetal osteoblast (hFOB) cell line (Figure 7E). Further studies are needed to determine if inhibition of JAB1 using CSN5i-3 can overcome radio and chemotherapy resistance in OS, similarly to reports of *JAB1* knockdown in nasopharyngeal carcinoma and OS cells (38, 42, 43).

We also found that CSN5i-3 and MLN4924 also differentially affect two CRL F-box proteins, FBXO22 and SKP2 (Figure 7E). SKP2, as a well-studied F-Box protein, is an established oncogene that is overexpressed in OS cells, and its downregulation inhibits OS cell growth and metastasis *in vitro* and *in vivo* (37, 44). Interestingly, MLN4924 treatment in fact increased the expression of SKP2, whereas CSN5i-3 treatment decreased its expression OS cells (Figure 7E). In contrast to SKP2, much less is known about FBXO22, which has both a positive and negative role in breast cancer progression and metastasis, respectively (45). Furthermore, *Fbxo22*-depletion resulted in the reduced response of ER-positive breast cancer cells to tamoxifen, and the overexpression of *JAB1* has been shown to confer tamoxifen resistance in ER-positive breast cancer (46, 47). In our study, CSN5i-3 treatment completely abolished FBXO22 expression (Figure 7E). Thus, our results and others indicate that FBXO22 may be a unique target of CSN5i-3 and JAB1 in OS and other cancers. The specific role of FBXO22 in cancer cells, especially identification of its downstream substrates involved in oncogenesis, remains to be elucidated to facilitate our understanding of the mechanism controlling JAB1-mediated cancer pathogenesis. While our present study demonstrates that CSN5i-3's inhibition of JAB1 may be suitable for the treatment of OS, further studies are necessary to address its *in vivo* efficacy in treating OS patients.

Materials and Methods

Complete and detailed materials and methods may be found in the Supplementary Materials.

Antibodies

The antibodies and antibody dilutions used in this study are listed in Supplementary Table S4.

Transgenic Construct

The full-length FLAG-tagged *Jab1* cDNA was cloned into a *Col1a1*-WPRE transgenic expression vector as described previously (30). Mice were maintained on a FVB/N background, and genotyping was performed as previously described (13). *Tp53* heterozygous mice were maintained as previously described (4).

RNA-sequencing

Total RNAs were isolated from control and *JAB*-knockdown 143B cells as described (48). $N = 3$ each for each group. RNA-sequencing was performed at the Genomics Core at Case Western Reserve University. The dataset has been deposited into the NCBI Gene Expression Omnibus under the accession number GSE117773.

Supplementary Material

Refer to Web version on PubMed Central for supplementary material.

Acknowledgements

The authors thank Teresa Pizzuto for her expert histology work. We also thank Dr. Eva Altmann (Novartis) for the generous gift of CSN5i-3. This study was supported in part by the NCI R03 CA175874, the American Cancer Society Research Grant #119999-IRG-91-022-IRG, and the National Institute of Arthritis and Musculoskeletal and Skin Diseases of the National Institutes of Health R01 AR068361 to G.Z., and the T32 AR007505 to W.E.S. and L.A.B., as well as the Rally Foundation for Childhood Cancer Research and Open Hands Overflowing Hearts Fellowship to W.E.S. under award ID CON221575. This research was supported by the Cytometry & Imaging Microscopy Shared Resource of the Case Comprehensive Cancer Center (P30CA043703) and the Genomics Core Facility of the CWRU School of Medicine's Genetics and Genome Sciences Department. The content of this study is solely the responsibility of the authors and does not necessarily represent the official views of the National Institutes of Health.

Financial Support: NCI R03 CA175874 to G.Z., ACS #119999-IRG-91-022-18-IRG to G.Z., NIAMS R01 AR068361 to G.Z., NIAMS T32 AR7505-30 to W.E.S. and L.A.B., and the Rally Foundation for Childhood Cancer Research and Open Hands Overflowing Hearts Fellowship CON221575 to W.E.S.

REFERENCES

1. Mirabello L, Troisi RJ, Savage SA. Osteosarcoma incidence and survival rates from 1973 to 2004: data from the Surveillance, Epidemiology, and End Results Program. *Cancer*. 2009;115(7):1531–43. [PubMed: 19197972]
2. Gianferante DM, Mirabello L, Savage SA. Germline and somatic genetics of osteosarcoma - connecting aetiology, biology and therapy. *Nat Rev Endocrinol*. 2017;13(8):480–91. [PubMed: 28338660]
3. Donehower LA, Harvey M, Slagle BL, McArthur MJ, Montgomery CA Jr., Butel JS, et al. Mice deficient for p53 are developmentally normal but susceptible to spontaneous tumours. *Nature*. 1992;356(6366):215–21. [PubMed: 1552940]

4. Jacks T, Remington L, Williams BO, Schmitt EM, Halachmi S, Bronson RT, et al. Tumor spectrum analysis in p53-mutant mice. *Curr Biol*. 1994;4(1):1–7. [PubMed: 7922305]
5. Lin PP, Pandey MK, Jin F, Raymond AK, Akiyama H, Lozano G. Targeted mutation of p53 and Rb in mesenchymal cells of the limb bud produces sarcomas in mice. *Carcinogenesis*. 2009;30(10):1789–95. [PubMed: 19635748]
6. Walkley CR, Qudsi R, Sankaran VG, Perry JA, Gostissa M, Roth SI, et al. Conditional mouse osteosarcoma, dependent on p53 loss and potentiated by loss of Rb, mimics the human disease. *Genes & development*. 2008;22(12):1662–76. [PubMed: 18559481]
7. Berman SD, Calo E, Landman AS, Danielian PS, Miller ES, West JC, et al. Metastatic osteosarcoma induced by inactivation of Rb and p53 in the osteoblast lineage. *P Natl Acad Sci USA*. 2008;105(33):11851–6.
8. Kato JY, Yoneda-Kato N. Mammalian COP9 signalosome. *Genes Cells*. 2009;14(11):1209–25. [PubMed: 19849719]
9. Liu G, Claret FX, Zhou F, Pan Y. Jab1/COP5 as a Novel Biomarker for Diagnosis, Prognosis, Therapy Prediction and Therapeutic Tools for Human Cancer. *Front Pharmacol*. 2018;9:135. [PubMed: 29535627]
10. Wei N, Serino G, Deng XW. The COP9 signalosome: more than a protease. *Trends Biochem Sci*. 2008;33(12):592–600. [PubMed: 18926707]
11. Claret FX, Hibi M, Dhut S, Toda T, Karin M. A new group of conserved coactivators that increase the specificity of AP-1 transcription factors. *Nature*. 1996;383(6599):453–7. [PubMed: 8837781]
12. Bashur LA, Chen D, Chen Z, Liang B, Pardi R, Murakami S, et al. Loss of jab1 in osteochondral progenitor cells severely impairs embryonic limb development in mice. *J Cell Physiol*. 2014;229(11):1607–17. [PubMed: 24604556]
13. Chen D, Bashur LA, Liang B, Panattoni M, Tamai K, Pardi R, et al. The transcriptional co-regulator Jab1 is crucial for chondrocyte differentiation in vivo. *J Cell Sci*. 2013;126(Pt 1):234–43. [PubMed: 23203803]
14. Sitte S, Glasner J, Jellusova J, Weisel F, Panattoni M, Pardi R, et al. JAB1 is essential for B cell development and germinal center formation and inversely regulates Fas ligand and Bcl6 expression. *J Immunol*. 2012;188(6):2677–86. [PubMed: 22327073]
15. Panattoni M, Sanvito F, Basso V, Doglioni C, Casorati G, Montini E, et al. Targeted inactivation of the COP9 signalosome impairs multiple stages of T cell development. *J Exp Med*. 2008;205(2):465–77. [PubMed: 18268034]
16. Oh W, Lee EW, Sung YH, Yang MR, Ghim J, Lee HW, et al. Jab1 induces the cytoplasmic localization and degradation of p53 in coordination with Hdm2. *J Biol Chem*. 2006;281(25):17457–65. [PubMed: 16624822]
17. Lauvrak SU, Munthe E, Kresse SH, Stratford EW, Namlos HM, Meza-Zepeda LA, et al. Functional characterisation of osteosarcoma cell lines and identification of mRNAs and miRNAs associated with aggressive cancer phenotypes. *Br J Cancer*. 2013;109(8):2228–36. [PubMed: 24064976]
18. Collier CD, Wirtz EC, Knafler GJ, Morris WZ, Getty PJ, Greenfield EM. Micrometastatic Drug Screening Platform Shows Heterogeneous Response to MAP Chemotherapy in Osteosarcoma Cell Lines. *Clin Orthop Relat Res*. 2018.
19. Ottaviano L, Schaefer KL, Gajewski M, Huckenbeck W, Baldus S, Rogel U, et al. Molecular characterization of commonly used cell lines for bone tumor research: a trans-European EuroBoNet effort. *Genes Chromosomes Cancer*. 2010;49(1):40–51. [PubMed: 19787792]
20. Behjati S, Tarpey PS, Haase K, Ye H, Young MD, Alexandrov LB, et al. Recurrent mutation of IGF signalling genes and distinct patterns of genomic rearrangement in osteosarcoma. *Nat Commun*. 2017;8:15936. [PubMed: 28643781]
21. Perry JA, Kiezun A, Tonzi P, Van Allen EM, Carter SL, Baca SC, et al. Complementary genomic approaches highlight the PI3K/mTOR pathway as a common vulnerability in osteosarcoma. *Proc Natl Acad Sci U S A*. 2014;111(51):E5564–73. [PubMed: 25512523]
22. Zhang F, Yan T, Guo W, Sun K, Wang S, Bao X, et al. Novel oncogene COPS3 interacts with Beclin1 and Raf-1 to regulate metastasis of osteosarcoma through autophagy. *J Exp Clin Cancer Res*. 2018;37(1):135. [PubMed: 29970115]

23. Crone SG, Jacobsen A, Federspiel B, Bardram L, Krogh A, Lund AH, et al. microRNA-146a inhibits G protein-coupled receptor-mediated activation of NF-kappaB by targeting CARD10 and COPS8 in gastric cancer. *Mol Cancer*. 2012;11:71. [PubMed: 22992343]
24. Lee YH, Judge AD, Seo D, Kitade M, Gomez-Quiroz LE, Ishikawa T, et al. Molecular targeting of CSN5 in human hepatocellular carcinoma: a mechanism of therapeutic response. *Oncogene*. 2011;30(40):4175–84. [PubMed: 21499307]
25. Huang da W, Sherman BT, Lempicki RA. Systematic and integrative analysis of large gene lists using DAVID bioinformatics resources. *Nat Protoc*. 2009;4(1):44–57. [PubMed: 19131956]
26. Huang da W, Sherman BT, Lempicki RA. Bioinformatics enrichment tools: paths toward the comprehensive functional analysis of large gene lists. *Nucleic Acids Res*. 2009;37(1):1–13. [PubMed: 19033363]
27. Ballatori SE, Hinds PW. Osteosarcoma: prognosis plateau warrants retinoblastoma pathway targeted therapy. *Signal Transduct Target Ther*. 2016;1:16001. [PubMed: 29263893]
28. Loukil A, Cheung CT, Bendris N, Lemmers B, Peter M, Blanchard JM. Cyclin A2: At the crossroads of cell cycle and cell invasion. *World J Biol Chem*. 2015;6(4):346–50. [PubMed: 26629317]
29. Gavet O, Pines J. Progressive activation of CyclinB1-Cdk1 coordinates entry to mitosis. *Dev Cell*. 2010;18(4):533–43. [PubMed: 20412769]
30. Zhou G, Zheng Q, Engin F, Munivez E, Chen Y, Sebald E, et al. Dominance of SOX9 function over RUNX2 during skeletogenesis. *Proc Natl Acad Sci U S A*. 2006;103(50):19004–9. [PubMed: 17142326]
31. Tao J, Jiang MM, Jiang L, Salvo JS, Zeng HC, Dawson B, et al. Notch activation as a driver of osteogenic sarcoma. *Cancer Cell*. 2014;26(3):390–401. [PubMed: 25203324]
32. Enchev RI, Schulman BA, Peter M. Protein neddylation: beyond cullin-RING ligases. *Nat Rev Mol Cell Biol*. 2015;16(1):30–44. [PubMed: 25531226]
33. Malhab LJ, Descamps S, Delaval B, Xirodimas DP. The use of the NEDD8 inhibitor MLN4924 (Pevonedistat) in a cyclotherapy approach to protect wild-type p53 cells from MLN4924 induced toxicity. *Sci Rep*. 2016;6:37775. [PubMed: 27901050]
34. Soucy TA, Smith PG, Milhollen MA, Berger AJ, Gavin JM, Adhikari S, et al. An inhibitor of NEDD8-activating enzyme as a new approach to treat cancer. *Nature*. 2009;458(7239):732–6. [PubMed: 19360080]
35. Zhou L, Jiang Y, Luo Q, Li L, Jia L. Neddylation: a novel modulator of the tumor microenvironment. *Mol Cancer*. 2019;18(1):77. [PubMed: 30943988]
36. Schlierf A, Altmann E, Quancard J, Jefferson AB, Assenberg R, Ratus M, et al. Targeted inhibition of the COP9 signalosome for treatment of cancer. *Nat Commun*. 2016;7:13166. [PubMed: 27774986]
37. Wang Z, Liu P, Inuzuka H, Wei W. Roles of F-box proteins in cancer. *Nat Rev Cancer*. 2014;14(4):233–47. [PubMed: 24658274]
38. Tian L, Peng G, Parant JM, Leventaki V, Drakos E, Zhang Q, et al. Essential roles of Jab1 in cell survival, spontaneous DNA damage and DNA repair. *Oncogene*. 2010;29(46):6125–37. [PubMed: 20802511]
39. Mori M, Yoneda-Kato N, Yoshida A, Kato JY. Stable form of JAB1 enhances proliferation and maintenance of hematopoietic progenitors. *J Biol Chem*. 2008;283(43):29011–21. [PubMed: 18667426]
40. Swords RT, Watts J, Erba HP, Altman JK, Maris M, Anwer F, et al. Expanded safety analysis of pevonedistat, a first-in-class NEDD8-activating enzyme inhibitor, in patients with acute myeloid leukemia and myelodysplastic syndromes. *Blood Cancer J*. 2017;7(2):e520. [PubMed: 28157218]
41. Manasanch EE, Orlowski RZ. Proteasome inhibitors in cancer therapy. *Nat Rev Clin Oncol*. 2017;14(7):417–33. [PubMed: 28117417]
42. Pan Y, Zhang Q, Atsaves V, Yang H, Claret FX. Suppression of Jab1/CSN5 induces radio- and chemo-sensitivity in nasopharyngeal carcinoma through changes to the DNA damage and repair pathways. *Oncogene*. 2013;32(22):2756–66. [PubMed: 22797071]
43. Pan Y, Wang S, Su B, Zhou F, Zhang R, Xu T, et al. Stat3 contributes to cancer progression by regulating Jab1/Csn5 expression. *Oncogene*. 2017;36(8):1069–79. [PubMed: 27524414]

44. Zhang Y, Zvi YS, Batko B, Zaphiros N, O'Donnell EF, Wang J, et al. Down-regulation of Skp2 expression inhibits invasion and lung metastasis in osteosarcoma. *Sci Rep.* 2018;8(1):14294. [PubMed: 30250282]
45. Sun R, Xie HY, Qian JX, Huang YN, Yang F, Zhang FL, et al. FBXO22 Possesses Both Protumorigenic and Antimetastatic Roles in Breast Cancer Progression. *Cancer Res.* 2018;78(18):5274–86. [PubMed: 29945959]
46. Johmura Y, Maeda I, Suzuki N, Wu W, Goda A, Morita M, et al. Fbxo22-mediated KDM4B degradation determines selective estrogen receptor modulator activity in breast cancer. *J Clin Invest.* 2018;128(12):5603–19. [PubMed: 30418174]
47. Lu R, Hu X, Zhou J, Sun J, Zhu AZ, Xu X, et al. COPS5 amplification and overexpression confers tamoxifen-resistance in ERalpha-positive breast cancer by degradation of NCoR. *Nat Commun.* 2016;7:12044. [PubMed: 27375289]
48. Liang B, Cotter MM, Chen D, Hernandez CJ, Zhou G. Ectopic expression of SOX9 in osteoblasts alters bone mechanical properties. *Calcif Tissue Int.* 2012;90(2):76–89. [PubMed: 22143895]

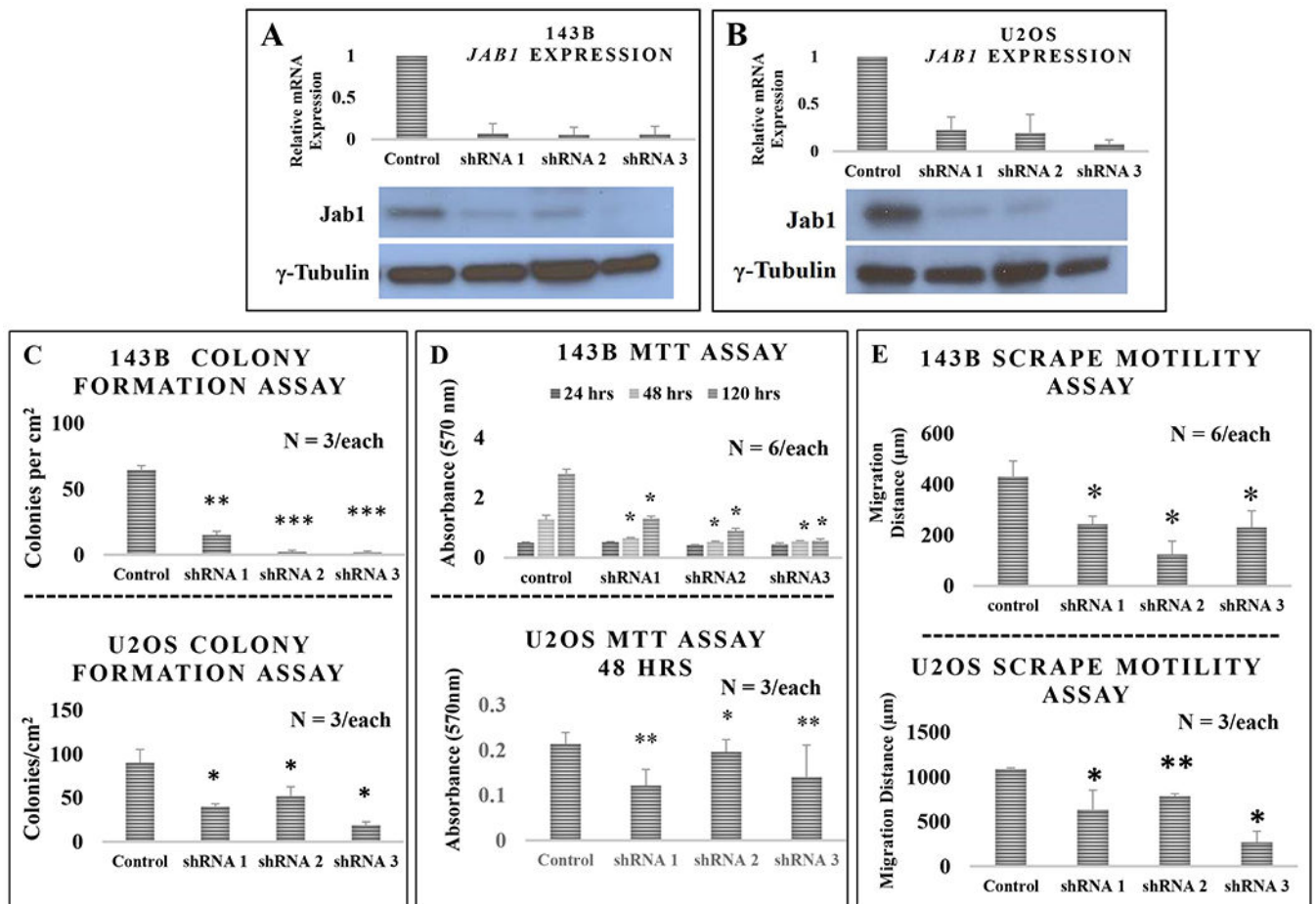


Figure 1. The downregulation of *JAB1* inhibits 143B and U2OS osteosarcoma cell growth *in vitro*. (A-B) The *JAB1* silencing efficiency was confirmed to be at least 80% by RT-qPCR and western blot analysis (n = 3). (C) The colony formation assay demonstrated that *JAB1*-knockdown significantly decreases the abilities of OS cells to form colonies (n = 3-6). (D) The MTT assay demonstrated that the *JAB1*-knockdown significantly decreased cell viability (n = 3-6). (E) The scrape motility assay demonstrated that *JAB1*-knockdown significantly inhibited cell migration (n = 3-6). Error bars represent means \pm SD. * p < 0.05, ** p < 0.01, *** p < 0.005. All controls in this experiment are a scrambled shRNA.

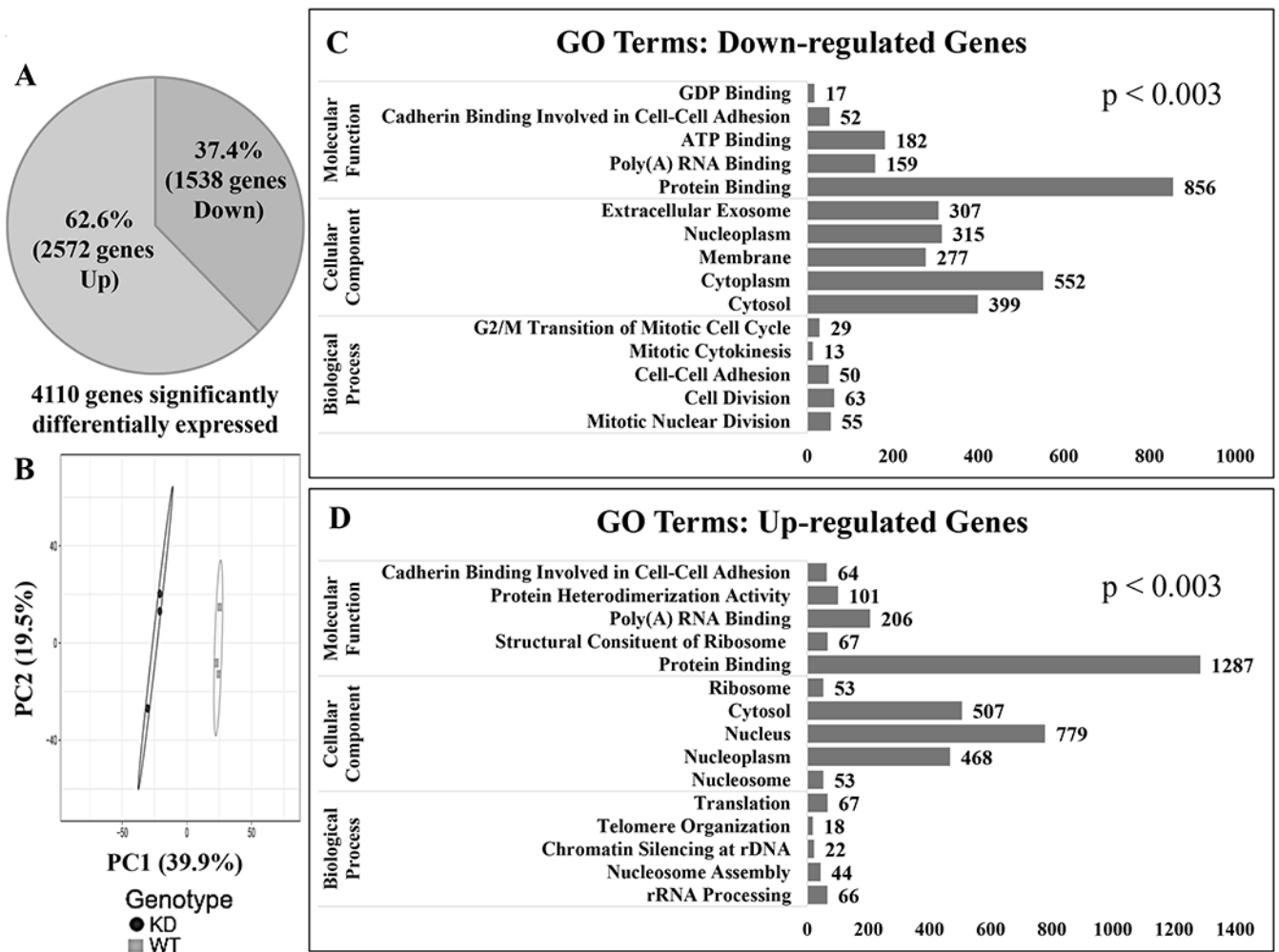


Figure 2. The RNA-seq analysis of *JABI*-depleted 143B human OS cells.

(A) The pie chart of significantly differentially expressed genes in *JABI*-knockdown versus control 143B cells. (B) The Principal Component Analysis identified the two distinct sets of genes that are differentially expressed in Wild-Type (WT, gray dots) vs. *JABI*-knockdown (KD, black dots) 143B cells. (C) Gene Ontology analysis list of the significantly downregulated genes and (D) upregulated genes using DAVID analysis. The x-axis denotes the number of genes. For all GO Terms presented here, $p < 0.003$.

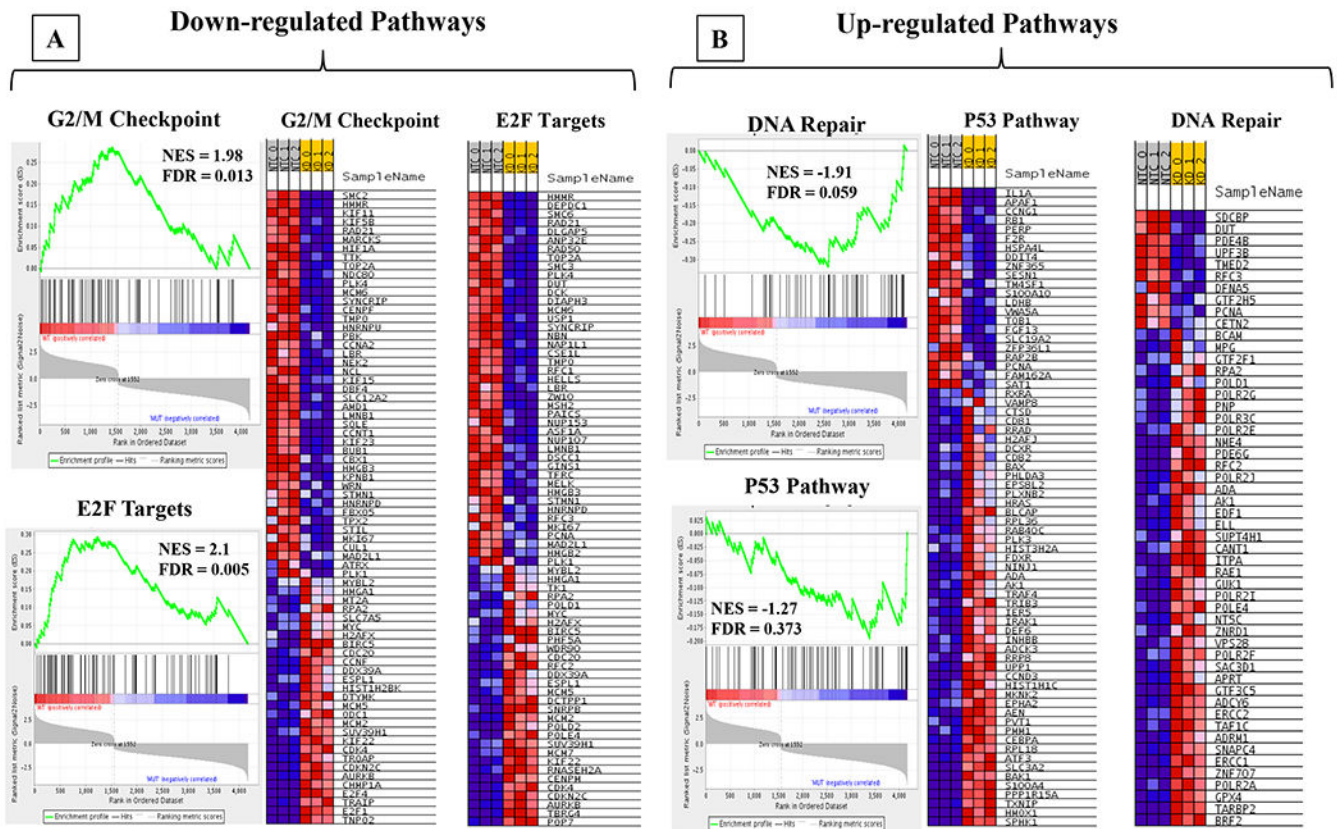


Figure 3. The Gene Set Enrichment Analysis identifies altered oncogenic pathways upon *JAB1*-knockdown in 143B OS cells.

(A) HALLMARK enrichment plots of G2/M checkpoint (NES = 1.98, FDR = 0.013) and E2F Targets (NES = 2.1, FDR = 0.005) gene sets (top left and bottom left panels) with the corresponding heat maps of these pathways at the right. (B) HALLMARK enrichment plots of the DNA repair (NES = -1.91, FDR = 0.059) and p53 (NES = -1.27, FDR = 0.373) pathways gene sets (top left and bottom left panels) with the corresponding heat maps of these pathways at the right.

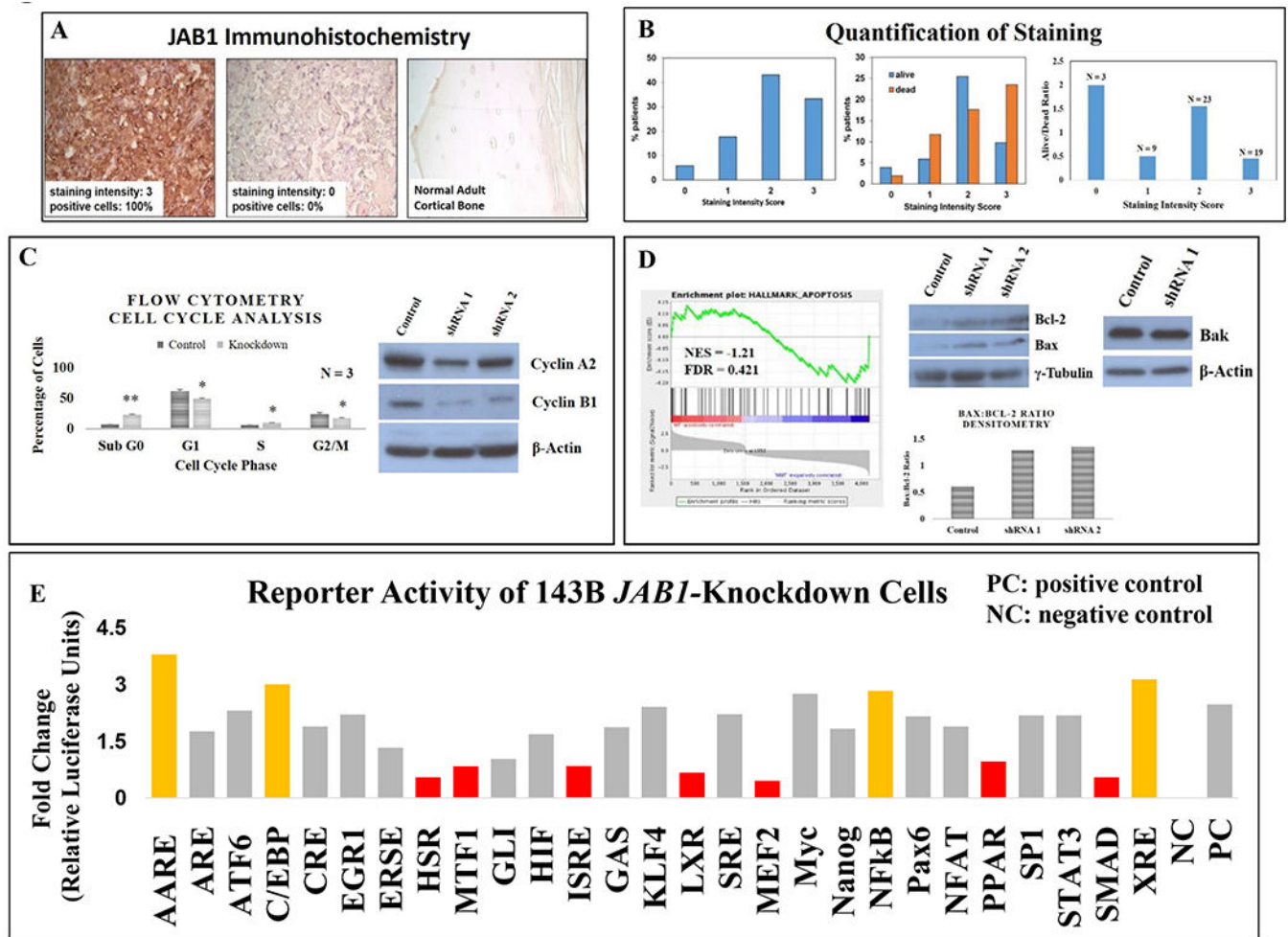


Figure 4. JAB1 is overexpressed in human OS biopsies, and *JAB1*-knockdown increases apoptosis and alters multiple major signal transduction pathways in OS cells. (A) The representative JAB1 immunohistochemistry of a human OS biopsy sample from an array of 51 samples, with a staining intensity score of 3 (left panel) and 0 (Middle panel). Right panel shows JAB1 immunohistochemistry in a normal human adult cortical bone sample. (B) Left panel, the percentage of each staining score across all samples. Middle panel, the staining intensity score was matched to the patient outcome. Right panel, the ratio of alive patients to dead patients for each staining intensity score. A lower number indicates poorer survival. (C) Left, the flow cytometry analysis of cell cycle in control and *JAB1*-knockdown 143B cells. Error bars represent means \pm SD (n = 3). Right, western blotting demonstrates decreased expression of Cyclin A2 and Cyclin B1. (D) Left, The GSEA identifies the apoptosis pathway (NES = -1.21, FDR = 0.421) as being upregulated in *JAB1*-knockdown 143B cells. Right, Western blotting demonstrates increased expressions of Bax and Bcl-2, but not Bak, in 143B *JAB1*-knockdown cells. Densitometry analysis of the Bax:Bcl-2 ratio. (E) The Signal Reporter Assay in *JAB1*-knockdown 143B cells. Red bars indicate all of the downregulated pathways; yellow bars indicate the top 4 most upregulated pathways. A detailed list of pathways is listed in Supplementary Table S3.

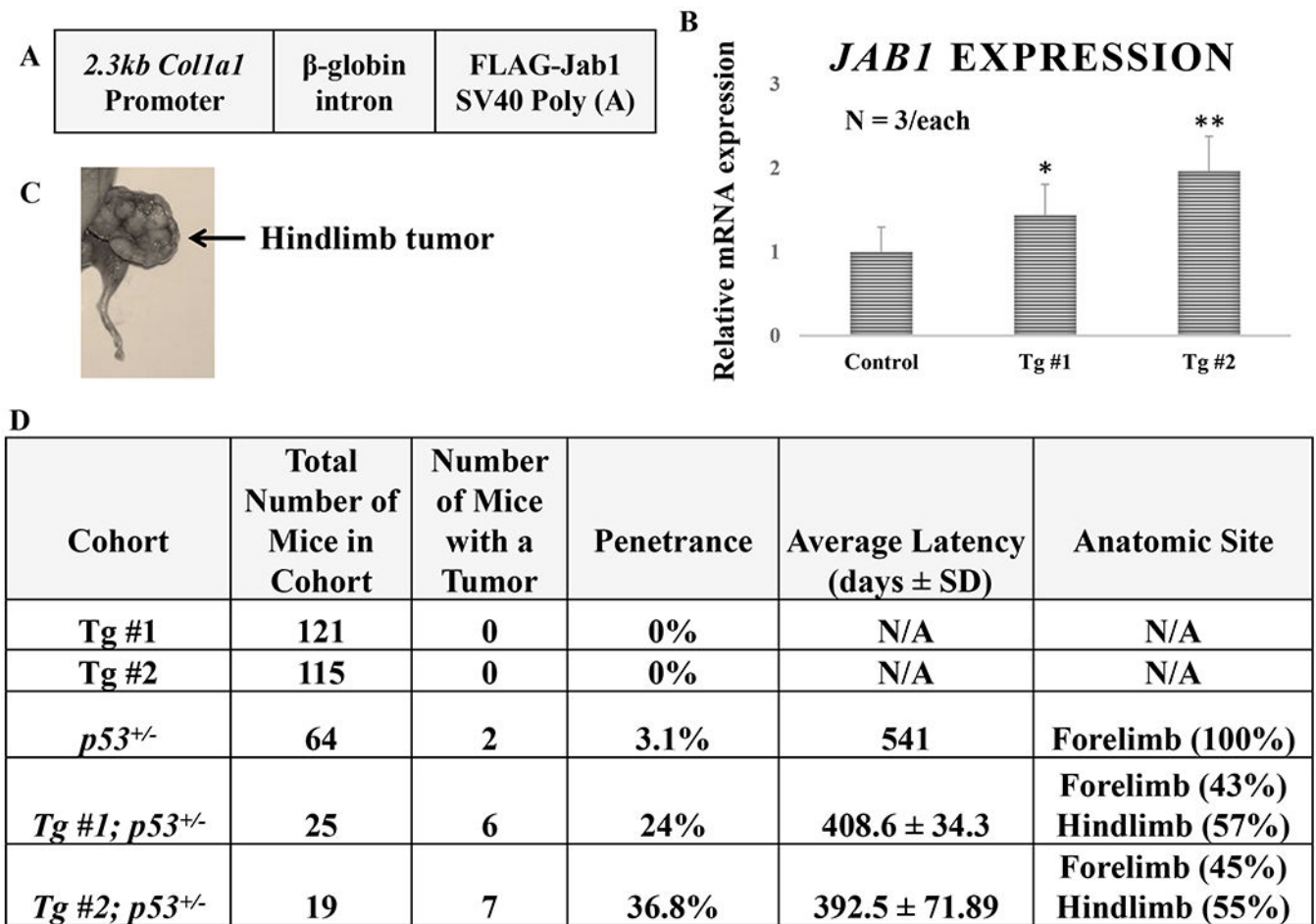


Figure 5. The osteoblast-specific overexpression of *Jab1* results in accelerated, spontaneous, *p53*-dependent OS formation in mice.

(A) The schematic representation of the construct used to generate *Coll1a1-Jab1* transgenic mice. (B) The RT-qPCR analysis of *Jab1* expression from 8-week-old long bones of control and 2 independent *Coll1a1-Jab1* mouse transgenic lines (n = 3). (C) The representative image of a hindlimb tumor from a *Coll1a1-Jab1; p53*^{+/-} transgenic mouse. (D) The summary table of the different cohorts of mice used in this study and their OS occurrence. Tg, Transgenic

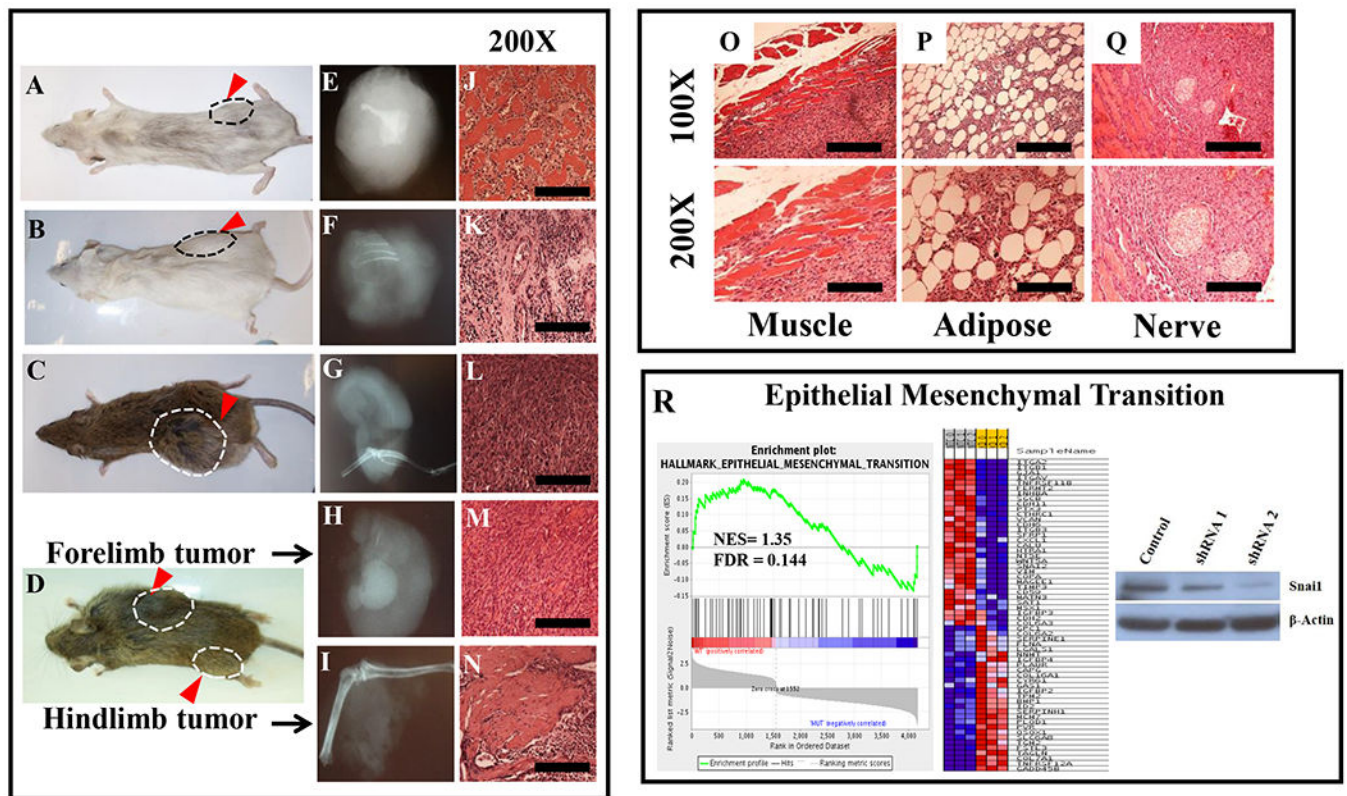


Figure 6. The characterization of spontaneous OS tumors in *Colla1-Jab1*; *p53*^{+/-} mice. (A-D) Representative images of mice that formed bone tumors, with dotted lines outlining the tumors. (E-I) X-ray analysis of those tumors, and (J-N) corresponding H&E staining of the tumors at 200x magnification. Scale bars, 50 μm. Histology revealed the local invasion of OS cells into the (O) surrounding muscle and (P) adipose, but not (Q) nerve tissue. Scale bars, 100X, 100 μm, 200X, 50 μm. (R) (Left) The HALLMARK GSEA enrichment plot and the heat map of Epithelial Mesenchymal Transition pathway (NES = 1.35, FDR = 0.144), (Right) Western blot analysis of SNAI1 in *JAB1*-knockdown 143B OS cells.

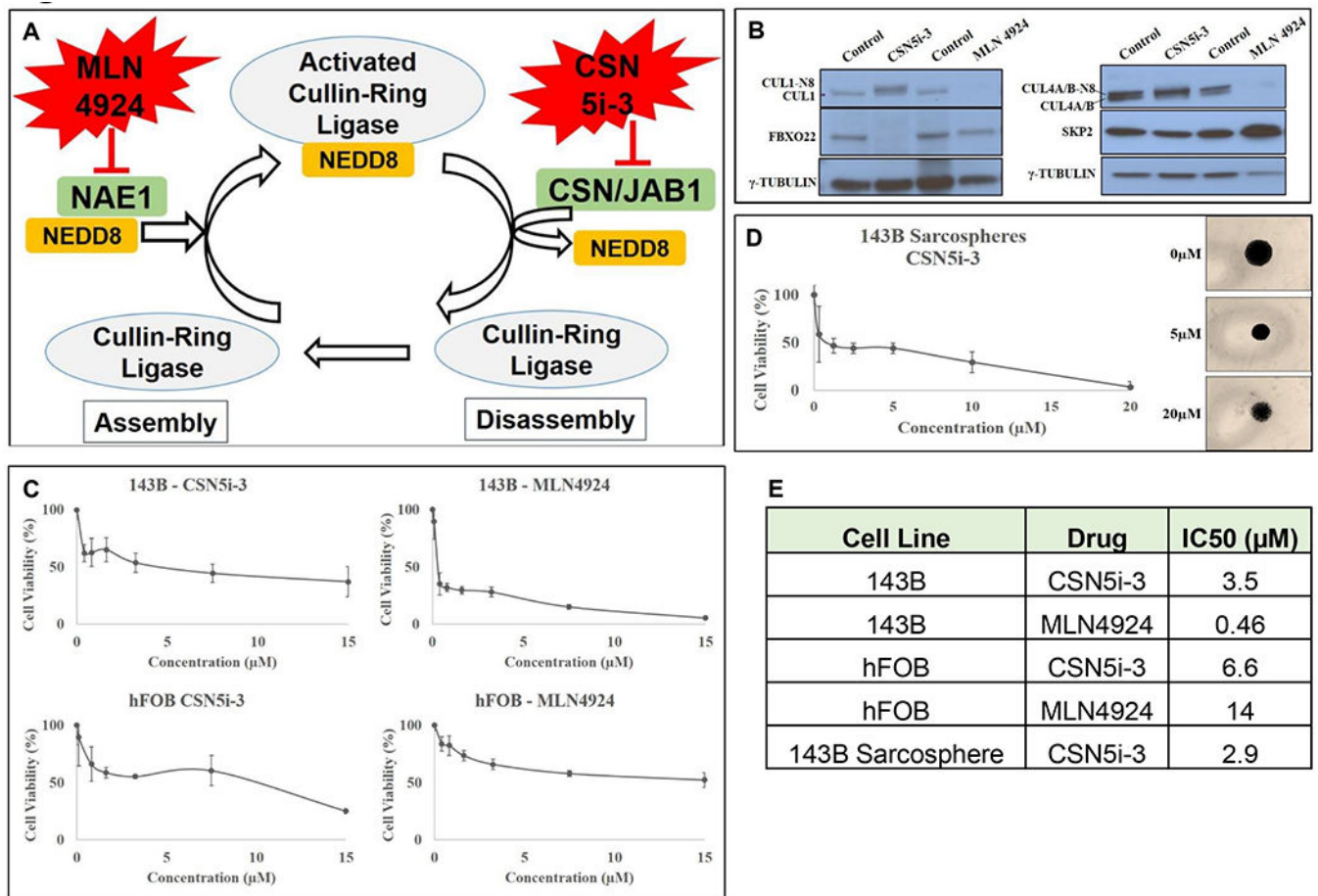


Figure 7. JAB1 is a potential therapeutic target in osteosarcoma.

(A) Schematic representation of Cullin-RING Ligase (CRL) activation by NAE1 and inactivation by JAB1, and the effects of MLN4924 and CSN5i-3 on CRL homeostasis. (B) Western blot analysis of 143B cells treated with CSN5i-3 or MLN4924 demonstrated their differential effects on representative CRL Cullin and F-Box proteins. (C) Dose-response curves showing the cell viability of 143B cells (top) and hFOB cells (bottom) treated with CSN5i-3 (left) and MLN4924 (right) for 48 hours. Each point in each graph represents mean \pm SD of 6 technical replicates. Representative curves from two independent experiments with similar results are shown for each cell line and drug (D) Left, dose-response curve showing the cell viability of 143B sarcospheres treated with CSN5i-3 for 48 hours. Each point represents mean \pm SD for 6 technical replicates. A representative curve from two independent experiments is shown. Right, representative pictures of 143B sarcospheres treated with 0, 5, and 20 μM CSN5i-3 for 48 hours. (E) IC50 Table.